



EUROPEAN ORGANIZATION FOR NUCLEAR RESEARCH

CERN/INTC 2000-038/

INTC/P132

30-Oct-00

PROPOSAL TO THE ISOLDE COMMITTEE

Studies of Colossal Magnetoresistive Oxides with Radioactive Isotopes

Aveiro¹, Grenoble², Leipzig³, Leuven⁴, Lisboa⁵, Orsay⁶, Porto⁷, Sacavém⁸, Stuttgart⁹, Tokyo¹⁰, Tsukuba¹¹ and CERN¹²
Collaboration

E. Alves⁸, V.S. Amaral¹, J.P. Araújo⁷, T. Butz³, J.G. Correia^{8,12}, C. Dubourdieu², H.-U. Habermeier⁹, A.A.Lourenço¹, J.G. Marques^{5,8}, M.F. da Silva^{5,8}, J.P. Senateur², J.C. Soares^{5,8}, J.B. Sousa⁷, R. Suryan⁶, Y. Tokura¹⁰, P.B. Tavares¹, Y. Tomioka¹¹, W.Tröger³, A. Vantomme⁴, J.M. Vieira¹, U. Wahl⁴ and F. Weiss².

Spokesman: V. S. Amaral, Contact person: J.G. Correia

ABSTRACT

We propose to study Colossal Magnetoresistive (CMR) oxides with several nuclear techniques, which use radioactive elements at ISOLDE. Our aim is to provide local and element selective information on some of the doping mechanisms that rule electronic interactions and magneto-resistance, in a complementary way to the use of conventional characterisation techniques. Three main topics are proposed:

- a) Studies of local [charge and] structural modifications in antiferromagnetic $\text{LaMnO}_{3+\delta}$ and $\text{La}_{1-x}\text{R}_x\text{MnO}_3$ with $\text{R}=\text{Ca}$ and Cd , doped ferromagnetic systems with competing interactions: - research on the lattice site and electronic characterisation of the doping element.
- b) Studies of self doped $\text{La}_{x-1-x}\text{MnO}_{3+\delta}$ systems, with oxygen and cation non- stoichiometry: -learning the role of defects in the optimisation of magnetoresistive properties.
- c) Probing the disorder and quenched random field effects in the vicinity of the charge or orbital Ordered/Ferromagnetic phase instability: - Investigating the local environment of ions at the Mn site, which trigger the ferromagnetic phase.

Our approach to study these problems, combines complementary techniques such as Perturbed Angular Correlation, Emission Channeling and Electrical/Magnetic Measurements in pellets, single crystals and high quality thin films of CMR oxides doped with radioactive isotopes. Preliminary results obtained in La Cd MnO_{3+x} pellets and thin films implanted with $^{111\text{m}}\text{Cd}$ are also presented.

¹Phys. Dept., Univ. Aveiro, P-3810 Aveiro, Portugal; ² UMR CNRS 5628, INPG-ENSPG, BP 46-38402 St. Martin D'Hères CEDEX, France; ³Fakultät für Physik und Geowissenschaften, Univ. Leipzig, Linnéstraße 5, D-04103 Leipzig, Germany; ⁴IKS, Celestijnenlaan 200 D, B-3001 Leuven, Belgium; ⁵CFNUL, Av. Prof. Gama Pinto 2, P-1699 Lisboa Codex, Portugal; ⁶Laboratoire Chimie des Solides, Université Paris Sud, 91405 Orsay Cedex, France, ⁷IFIMUP, Fac. Ciências, Rua do Campo Alegre 657, P-4150 Porto, Portugal; ⁸Instituto Tecnológico e Nuclear, E.N. 10, P-2685 Sacavém, Portugal; ⁹Max-Planck-Institut für Festkörperforschung, D70506 Stuttgart, Germany, ¹⁰Dep Applied Physics, Univ. Tokyo, Tokyo 113-86-56, Japan, ¹¹Joint Research Center for Atom Technology, Tsukuba 305-0046, Japan, ¹²EP Div., CERN, CH-1211 Geneva 23, Switzerland.

1 Motivation

1.1 Introduction

In the last six years an intense experimental [1] and theoretical [2] research has been devoted to the class of oxide materials, which present large changes of the electrical resistivity under the application of a magnetic field, the colossal magnetoresistive (CMR) manganese oxides. This is a class of strongly correlated electron systems, with many features similar to the high- T_c superconductors (HTSc). The relevant correlation mechanisms result from the close link between the magnetic coupling of manganese ions spins and the lattice and charge dynamics. These materials, often referred as manganites, have crystal structures derived from the cubic perovskite ABO_3 , where Mn occupies the B site and the A sites are occupied by rare-earth (La, Pr, Nd...) and other elements (Ca, Sr, Ba, Pb,...) (Figure 1).

The undoped $LaMnO_3$ compound is an antiferromagnetic insulator below $T_N \approx 140K$, due to antiferromagnetic (AF) superexchange interactions mediated by oxygen between manganese Mn^{3+} spins ($S=2$, due to strong Hund coupling). The cubic structure is distorted by cation size mismatch and the Jahn-Teller effect, leading to a distortion of the oxygen octahedron surrounding the B site cation which splits the upper e_g energy levels of a 3d ion such as Mn^{3+} , thus lowering the energy (Figure 1: top). The distorted structures are frequently orthorhombic or rhombohedral. When divalent ions are introduced at A-sites, some of the manganese ions become Mn^{4+} ($S=3/2$) and this favours a ferromagnetic interaction between 3+ and 4+ ion pairs. This interaction is referred as double-exchange (DE) [3] and results from the dynamic electron transfer across oxygen. The interesting point is that electron transfer from Mn^{3+} to Mn^{4+} is effective only if their core spins (from t_{2g} levels) are parallel. This brings a very close connection between ferromagnetic order and low electrical resistivity, resulting in very large magnetoresistance effects. Therefore, the Curie point coincides with a metal-insulator transition with anomalies in various physical

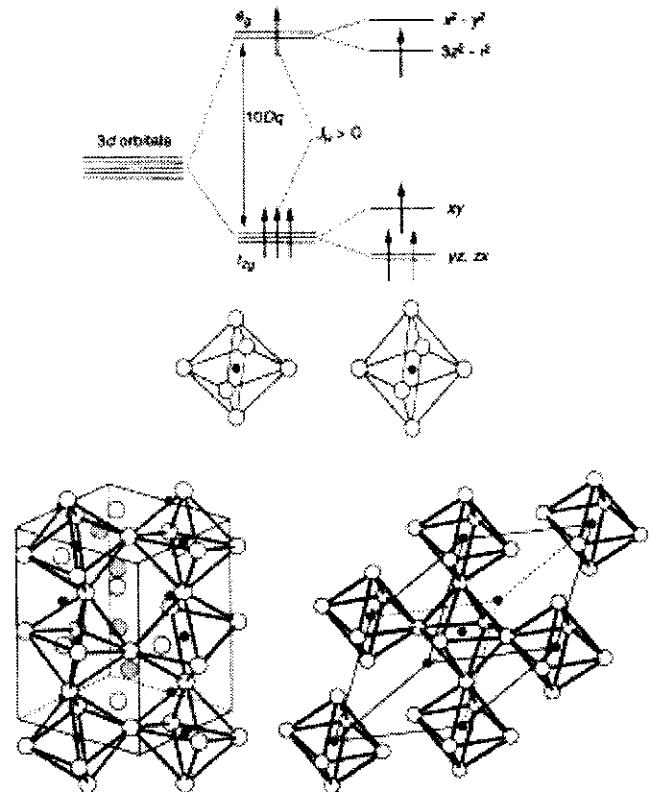


Figure 1 Crystal field and Jahn-Teller distortion of MnO_6 octahedral lead to splitting of d levels. Below: schematic orthorhombic and rhombohedral structures. Mn ions occupy the center of octahedral (B sites). (from ref [1]).

properties. It was soon recognised that the CMR oxides with rare-earth (such as lanthanum, praseodymium, neodymium, etc.) present a very rich variety of behaviours, associated with charge ordering (stripes), polaron formation and orbital ordering [4].

Like the case of high- T_C superconductors, where superconductivity arises from doping an antiferromagnetic insulator state, the CMR effects are very sensitive to small variations on atomic positions, local distortions, impurities and vacancies. This makes the magnetoresistive properties of the ferromagnetic manganites strongly dependent on the preparation conditions as well as after growth annealing treatments, which tune the doping, inducing the Mn^{3+}/Mn^{4+} mixed valence. In particular, it is found that the oxygen non-stoichiometry and the A-site vacancies can promote effective doping in thin films, leading to large CMR properties at room temperature [5]. Moreover, oxygen excess was also found to promote cation vacancies at both La and Mn sites, thus leading to self-doping [6]. The way the slender shifts in atomic structures, vacancies and interstitials interactions influence CMR properties is currently a topic of major interest.

From the applications point of view, a strong effort has been devoted to the optimisation of thin film properties, tuning the [sharp] magnetic transition close to room temperature for bolometric applications [7]. New perspectives for magnetic sensing are brought by exploiting the diffuse phase transition, close to the charge ordered insulator/ferromagnetic metal instability, which is induced by Cr impurities at the manganese site [8].

Traditional techniques (neutron diffraction, resonant X-ray scattering, diffuse X-ray scattering, Raman spectroscopy, scanning tunnelling spectroscopy, EXAFS [9] which are used to study the manganite structures are, however, not suitable to distinctly characterise the order/disorder and the interaction with point defects of both the lattice constituents and the dopant elements at an atomic scale.

Ion beams are being widely employed to analyse the composition, microstructure and to modify various properties of the CMR, HTSc and other oxide materials [10]. The characterisation of fundamental defect properties such as vacancies and interstitial elements [11], the ferromagnetic and charge ordering destruction by radiation damage [12], the introduction of tracers for diffusion, migration and trapping studies [13] established ion beam techniques as versatile tools for research in these materials.

Up to now, the specific advantages of nuclear spectroscopic techniques to study CMR Oxides are still far from being exploited. Studies using the Mössbauer Effect [14], Nuclear Magnetic Resonance [15] and, to a much lesser extent, Perturbed Angular Correlations (PAC) [16] were limited by the small number of adequate probe elements and by the sometimes difficult quality control of the sample preparation.

The development of the synthesis techniques [that represents alone a branch of research of some of the groups involved in this proposal] made nowadays available single-phase materials, high quality single crystals and thin films of the CMR oxide materials. Using such samples we propose a set of studies where the traditional characterisation techniques are combined with nuclear techniques commonly used at ISOLDE [17].

Three main subjects of inter-correlated research are proposed:

a) Studies of local [charge and] structural modifications in antiferromagnetic $\text{LaMnO}_{3+\delta}$ and $\text{La}_{1-x}\text{R}_x\text{MnO}_3$ with $\text{R}=\text{Ca}, \text{Cd}$, doped ferromagnetic systems with competing interactions: research on the lattice site and electronic characterisation of the doping element .

b) Studies of self doped $\text{La}_{1-x}\text{MnO}_{3+\delta}$ systems, with oxygen and cation non-stoichiometry, learning the role of defects in the optimisation of magnetoresistive properties.

c) Probing the disorder and quenched random field effects in the vicinity of the charge or orbital Ordered/Ferromagnetic phase instability. Investigating the local environment of Cr ions at the Mn site, which trigger the ferromagnetic phase.

1.2 Detailed Description

1.2.1 Local charge and structural modifications in antiferromagnetic $\text{LaMnO}_{3+\delta}$ and $\text{La}_{1-x}\text{R}_x\text{MnO}_3$ with $\text{R}=\text{Ca}$, Cd , doped ferromagnetic systems.

It is believed that doping effects in manganites are predominantly associated with the valence and size of the dopant ion. Considering this, the Cd doping would lead to ferromagnetic metallic behaviour as it is found with Ca. This was reported in an early study [18] but further work indicates that Cd leads to ferromagnetic insulator behaviour [19].

Figure 2 shows the different trend of the Curie temperature (T_C) of the paramagnetic-to-ferromagnetic transition as a function of the Ca and Cd doping.

Figure 3 shows the resistivity (ρ) and normalised magnetisation as a function of temperature on manganite samples doped with Ca and Cd. It is clearly seen the insulator-like behaviour of ρ in the case of the samples doped with Cd all-over the paramagnetic-to-ferromagnetic transition around 150K (*), in contrast to the metallic behaviour of Ca doped samples below T_C .

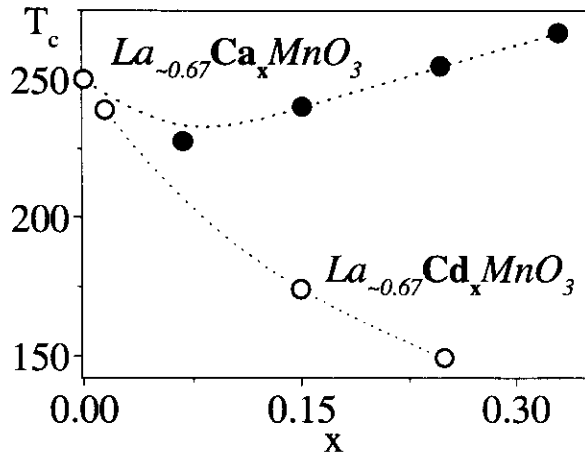


Figure 2 T_C measured as a function of temperature in $\text{La}_{0.67}\text{Ca}_x\text{MnO}_3$ and $\text{La}_{0.67}\text{Cd}_x\text{MnO}_3$ doped systems (*).

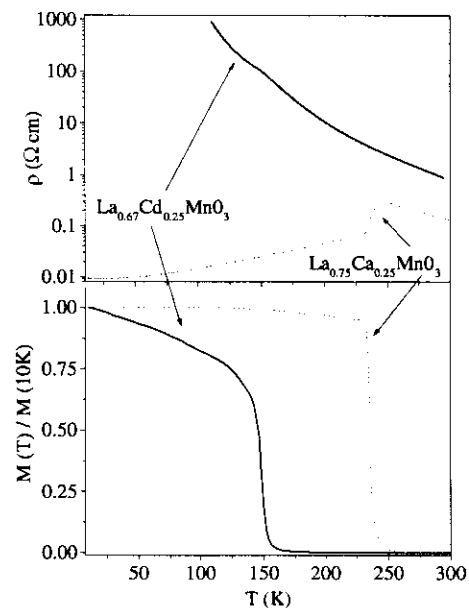


Figure 3 Resistivity (ρ) and magnetic susceptibility as a function of temperature on manganite samples doped with Ca and Cd (*).

So far two scenarios have been proposed to explain such features: i) Cd substitutes Mn and disrupts Mn-O-Mn DE interaction, like in the case of other transition metal doping (Fe, Cu, Zn, etc.) and ii) Cd substitutes La, promoting a charge redistribution that leads to ferromagnetic superexchange interactions Mn-O-Mn and insulating behaviour.

* The samples were produced and the measurements were done at Aveiro and Porto Universities, respectively.

A new insight on these topics can be achieved by studying the lattice site and the local electric and magnetic environment of Cd atoms in antiferromagnetic insulator and ferromagnetic (metallic or insulator) manganites.

For this purpose we propose to use the Perturbed Angular Correlation (PAC) and electron Emission Channeling (EC) techniques. PAC is particularly sensitive to the atomic vicinity of the probe's nuclei [20] and determines the Electric Field Gradient (EFG) and Magnetic Hyperfine Field (MHF) at the probe site. EC relies on the fact that charged particles emitted from radioactive isotopes in a single crystal experience channeling or blocking effects along low-index directions [21]. This leads to an anisotropic particle emission yield from the crystal surface, which depends in a characteristic way on the lattice sites occupied by the emitter atoms.

We intend to use the ^{111m}Cd (49 m) \rightarrow ^{111}Cd isotope, which is suitable for both γ - γ and e^- - γ PAC studies. Complementary studies onto decay from ^{117}Cd (2.4h) \rightarrow ^{117}In and ^{111}Ag (7.45d) \rightarrow ^{111}Cd PAC probe elements shall be done. The aim is to compare the hyperfine fields, which are measured with different probe elements, thus inferring the element-specific local behaviour on these lattices.

Figure 4 shows first PAC test experiments performed on the $\text{La}_{1-x}\text{Cd}_x\text{MnO}_3$ system implanted with ^{111m}Cd at ISOLDE. The $R(t)$ (PAC) spectrum, which is measured at room temperature, reveals an attenuated frequency that was fitted by assuming an EFG distribution most likely generated by the non stoichiometric material. The further attenuation of the low temperature spectrum [measured below the Curie temperature which is around 150K in this compound] has been fitted by only considering that a local magnetic field is acting now in addition to the same EFG field distribution that is measured at room temperature. The observable in such cases is described by considering combined magnetic and quadrupole interactions.

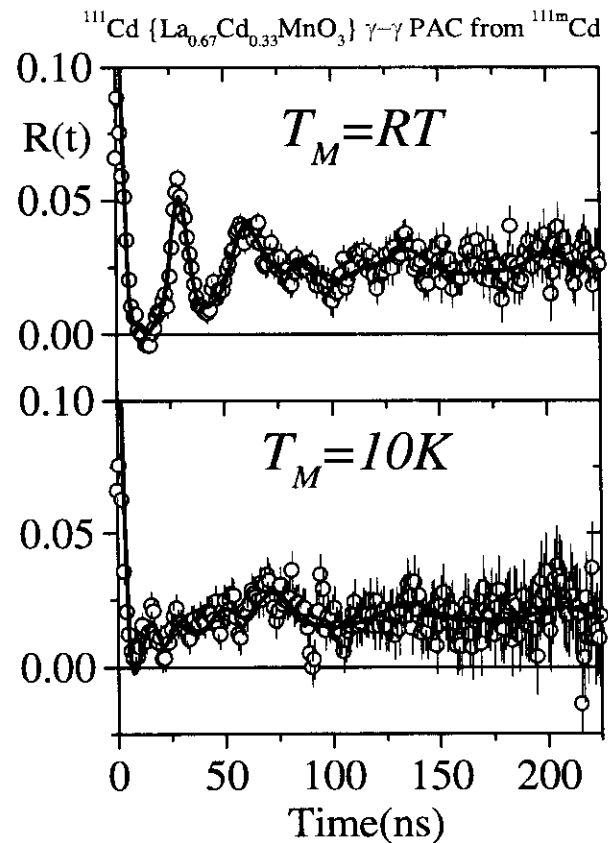


Figure 4 First test PAC measurement performed on $\text{La}_{1-x}\text{Cd}_x\text{MnO}_3$ ^{111m}Cd implanted systems. The attenuation of the low temperature spectrum is due to the presence of a magnetic field that is absent at room temperature.

The lattice site location of Cd and Ag will be studied by electron EC in single crystals and epitaxial thin films implanted with the $^{115}\text{Cd} (53.5\text{h}) \rightarrow ^{115}\text{In}$ and the $^{111}\text{Ag} (7.45\text{d}) \rightarrow ^{111}\text{Cd}$ isotopes. In these experiments β^- -particles from the $^{115}\text{Cd}/^{115}\text{In}$ and $^{111}\text{Ag}/^{111}\text{Cd}$ decay will be detected onto two-dimensional position sensitive Si pad detectors, which have been developed at CERN [21]. As example, Figure 5 shows the first EC test spectrum obtained from the decay of ^{115}Cd implanted in one $\text{La}_{0.75}\text{Ca}_{0.25}\text{MnO}_3$ thin film, epitaxial grown perpendicularly to the (001) surface. This data shows that Cd goes to substitutional lattice sites. However to find the Cd specific lattice, several EC measurements performed over different principal axes are required for each compound.

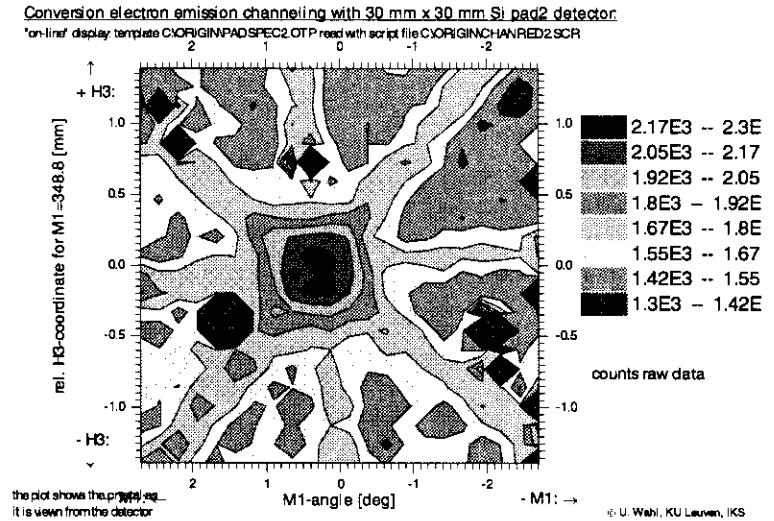


Figure 5 First EC test experiments performed on $\text{La}_{0.75}\text{Ca}_{0.25}\text{MnO}_3$

The radioactive isotopes will be implanted into pellets, single crystals and thin films of these materials and the PAC and EC studies will be performed after implantation and suitable annealing procedure. The measurements shall be done in a broad temperature range (10-1000K) to encompass the different magnetic and structural phase transitions, which shall be studied in detail.

1.2.2 Studies of self doped $\text{La}_x\text{Ca}_{1-x}\text{MnO}_{3+\delta}$ systems, with oxygen and cation non-stoichiometry.

$\text{LaMnO}_{3+\delta}$ and divalent cation doped manganites show particularly strong changes of T_C with oxygen excess δ , similarly to what is found in high- T_C superconductors for the critical temperature dependence with doping [5].

A first example of such effect is presented in Figure 6 for the $\text{La}_{0.815}\text{Sr}_{0.185}\text{MnO}_{3+\delta}$ compound, which shows a maximum ferromagnetic T_C transition for $\delta \approx 0.04$ [22]. Figure 7 shows measurements of the magnetisation as a function of temperature, made subsequently to consecutive oxygen annealing treatments at increasing temperatures on $\text{La}_{0.8}\text{MnO}_{3+\delta}$ thin films, which progressively lead to the increase of T_C [23].

Particularly, in manganite thin films with relative Mn excess ($\text{La}_x\text{Ca}_{1-x}\text{MnO}_{3+\delta}$ and $\text{La}_x\text{Ca}_y\text{Ca}_{1-x-y}\text{MnO}_{3+\delta}$) the further incorporation of oxygen during annealing leads to T_C much above

the maximum reachable T_C in the bulk. Apparently, the constrained lattice can accommodate higher oxygen doping levels, thus enhancing the magnetic interactions [23].

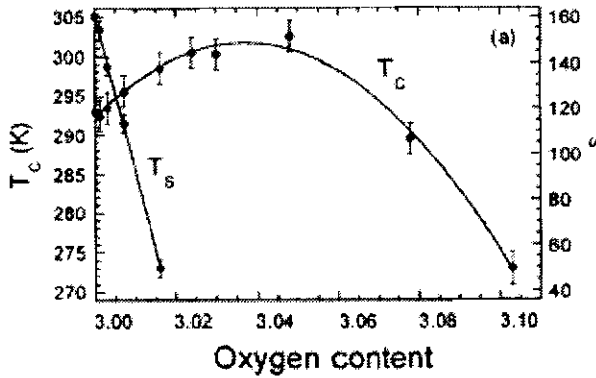


Figure 6 Curie temperature (T_C) dependence on oxygen content in $\text{La}_{0.815}\text{Sr}_{0.185}\text{MnO}_{3+\delta}$ (from ref [22]).

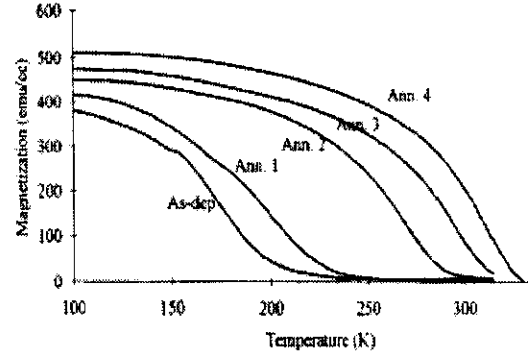


Figure 7 Temperature dependence of $\text{La}_{0.8}\text{MnO}_{3+\delta}$ thin films on subsequent oxygen annealing treatments that lead to the increase of T_C (from ref [23]).

We propose to use the ^{111m}Cd (49 m) \rightarrow ^{111}Cd PAC isotope, implanted into pellets and thin films of such materials, to probe the hyperfine fields, which depend on the doping effects from the oxygen incorporation and the cation vacancy formation. After low dose implantation and annealing in controlled atmosphere the PAC experiments will be performed from RT down to 10K. Looking forward to follow the dynamics of the oxygen incorporation further measurements should be done from RT up to 1000K after/during-annealing treatments in different atmospheres.

1.2.3 Disorder and quenched random field effects in the vicinity of the charge or orbital ordered/ferromagnetic phase instability.

Local electronic and lattice structure inhomogeneity often plays a crucial role in the properties of strongly correlated electron CMR and HTSc superconductor oxides. One of the most discussed points is, in particular, phase separation and the formation of charge and spin stripes [1,4]. In correlation with such effects, several near half-doped manganites exhibit huge magnetic field induced phenomena, which are due to the competition between the charge-orbital ordered (CO) insulating antiferromagnetic and the ferromagnetic metallic (FM) phase.

An example is presented in Figure 8 that shows the temperature dependence of resistivity of $\text{Pr}_{0.65}\text{Ca}_{0.35}\text{MnO}_3$ for several magnetic fields. There is clearly seen that the magnetic field triggers the transition from the CO- to the FM phase [24]. This phenomenon is extremely sensitive to the element species at the A-site. The FM phase appears when Ba or Sr replace some Ca, inducing local structural distortions that contribute to increase the conduction electron bandwidth.

More recently, a CO to FM phase transition was observed when introducing a small amount (few %) of Cr at the Mn sites [25]. This result is somewhat unexpected, since in ferromagnetic manganites (like $\text{La}_{0.67}\text{Ca}_{0.33}\text{MnO}_3$) Cr reduces the DE interaction, thus lowering T_C . This effect is supposed to be associated to a random field effect and the disorder disrupts the long range CO coherence, thus recovering the ferromagnetic phase. [26].

We propose to characterise the local environment of implanted Cr ions in several manganite systems. In addition, the sensitivity of the CO-FM transition to small doping concentrations suggest that resistivity measurements as a function of decay time of the implanted species may be possible.

Thin films of the undoped LaMnO_3 , ferromagnetic $\text{La}_{0.67}\text{Ca}_{0.33}\text{MnO}_3$ and charge-ordered $\text{La}_{0.5}\text{Ca}_{0.5}\text{MnO}_3$ and $\text{Pr}_{1-x}\text{Ca}_x\text{MnO}_3$ will be prepared with the most favourable stoichiometry to see the doping effect. We propose to implant ^{52}Mn (5.6d) \rightarrow ^{52}Cr , ^{140}La (1.7d) \rightarrow ^{140}Ce , ^{143}Ce (33h) \rightarrow ^{143}Pr , ^{153}Sm (47h) \rightarrow ^{153}Eu and ^{48}Cr (21.6h) \rightarrow ^{48}V . Our aim is to monitor precisely the effect of the element change on the electric and magnetic behaviour of the samples. β^+ and β^- emission channeling experiments will be performed to determine the lattice site of the implanted ^{52}Mn and ^{140}La . Studies of the local magnetic field can be performed with the ^{48}Cr (21.6h) \rightarrow ^{48}V , ^{143}Ce (33h) \rightarrow ^{143}Pr and ^{153}Sm (47h) \rightarrow ^{153}Eu PAC isotopes.

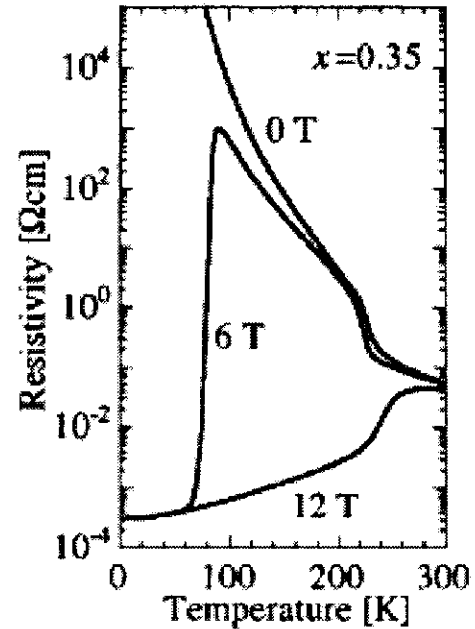


Figure 8 Electrical Resistivity observation of the magnetic field induced metal insulator transition in $\text{Pr}_{0.65}\text{Sr}_{0.35}\text{MnO}_{3+\delta}$ ([24]).

2. Experimental Facilities

2.1 Sample production

Table I: Where and how the samples are produced

Family of samples	Type of samples	Laboratory			
		Aveiro	Grenoble	Orsay	Stuttgart
La Mn O_3 + $\text{La}_{1-x}\text{R}_x\text{Mn O}_3$ $\text{R} = \text{Ca, Cd}$ + $\text{Pr}_{1-x}\text{Ca}_x\text{MnO}_3$	Pellets	Solid State Reaction	-	Solid State Reaction	-
	S. Crystals	Czochralski	-	Czochralski	-
	Thin films	Pulsed Laser Ablation	-	-	Pulsed Laser Ablation
$\text{La}_x\text{□}_{1-x}\text{Mn O}_{3+\delta}$	Pellets	-	-	Solid State Reaction	-
	Thin films	-	Metal Organic Chemical Vapour Deposition	-	-

2.2 Sample characterisation

All samples will be characterised using the techniques available at the home institutes before and after the experiments with radioactive isotopes. We mention X-ray powder and single crystal diffraction (Aveiro, Grenoble, Porto), grazing angle X-ray diffraction (Porto), Scanning Electron Microscopy (SEM) with Energy Dispersive X-ray (EDX) analysis (Aveiro, Grenoble), Transmission Electron Microscopy (TEM) and High Resolution TEM (Aveiro, Stuttgart), and Rutherford Backscattering/Channeling (RBS/C) (Lisboa/Sacavém). These techniques allow monitoring the sample's crystalline structure, orientation, composition, as well as the characterisation of the defects, implantation profile and residual damage from the ion implantation and annealing procedures. For comparison, similar samples will be implanted with higher doses of stable Cd, Cr, Mn, Ba and La at Sacavém, using the Danfysik-1090 high fluency ion implanter.

2.3 Techniques working with radioactive isotopes

Both the γ - γ and e^- - γ PAC techniques are well established at ISOLDE. The γ - γ PAC spectrometer allows measurements from 10K up to 1100 K under gas flow [27]. The e^- - γ PAC spectrometer allows measurements from 25K up to 873 K under vacuum [28].

The EC experiments are performed in the existing Lisbon and Leuven setups. These consist of vacuum chambers equipped with two-axes goniometers allowing in-situ heating (up to 1200 K) and cooling (down to 30 K). Electrons are detected on two-dimensional Si pad detectors developed at CERN [21].

Resistivity measurements performed as a function of temperature will be mainly done at CERN/ISOLDE with a closed cycle helium refrigerator (from Leipzig) equipped with a four contact resistivity probe head (from Porto). The measurement of the magnetic properties will be done using the ac-susceptibility and SQUID techniques at the home-institutes in Aveiro, Grenoble, Orsay, Porto and Stuttgart.

Table II: Radioactive isotopes and techniques

legend: PAC – Perturbed Angular Correlations

EC – Emission Channeling with beta particles (β , β^+) or conversion electrons (c.e.)

E & M – Measurement of Electric and Magnetic properties

isotope	annealing	γ - γ PAC	e^- - γ PAC	β - γ PAC	EC	E&M
^{111m}Cd (49 m) ↓ ^{111}Cd	✓	✓	✓	-	-	-
^{111}Ag (7.45 d) ↓ ^{111}Cd	✓	-	-	✓	✓	✓
^{115}Ag (20 m) ↓ ^{115}Cd (53.5 h) ↓ ^{115}In	implant & wait for decay ✓	-	-	-	-	-
^{117}Ag (73 s) ↓ ^{117}Cd (2.4 h) ↓ ^{117}In (1.9 h)	implant & wait for decay ✓	-	-	-	-	-
^{140}La (1.7 d) ↓ ^{140}Ce	✓	-	-	-	✓(β^-)	✓

Table II: Radioactive isotopes and techniques (*continuation from the previous page*)

isotope	annealing	γ - γ PAC	e^- - γ PAC	β - γ PAC	EC	E&M
^{143}Ce (33h) ↓	✓					
^{143}Pr (13.6d)	-	✓	-	-	-	-
^{153}Sm (47h) ↓	✓					
^{153}Eu	-	✓	-	-	✓(β^-)	-
^{52}Mn (5.6 d) ↓	✓					
^{52}Cr	-	-	-	-	✓(β^+)	✓
^{48}Cr (22 h) ↓	✓					
^{48}V (16 d)	-	✓	-	-	-	✓

3. Experimental requirements at ISOLDE

3.1 Laboratory

Collections of the isotopes should be done in the implantation chambers, which are currently available on GLM and GHM at the ISOLDE hall, building 170. All measurements will be done off-line, out of the ISOLDE hall, in radioactive *Class C* laboratories. The transport of samples inside CERN is made in vacuum-sealed plastic boxes.

e^- - γ and γ - γ PAC experiments are performed in room 304-R / 012. When PAC measurements under gas atmosphere are required the γ - γ PAC spectrometer will be mounted on room 3-1 / 039, as is currently used by the IS360 proposal.

The Emission Channeling experiments are actually running in room 304-R / 012 (Lisbon setup) and building 165 (Leuven Setup).

Resistivity measurements are done in room 304-R / 012.

Several furnace systems exist already at ISOLDE for annealing treatments under vacuum or gas flow at atmospheric pressure in room 3-1 / 39. All furnaces are equipped with activated charcoal filters that trap volatile elements.

3.2 Beam time request

We ask for 26 + 2-test shifts within the next two years according to Table III.

Table III: Beam time request

italic characters indicate optional target/ion sources

required isotope	implanted beam	intensity [at/ μ C]	target	ion source	number of shifts
^{111m}Cd	^{111m}Cd	$\sim 5 \times 10^8$	Molten Sn	plasma	12
$^{115}\text{Cd}, ^{115m}\text{Cd}$	$^{115}\text{Cd}, ^{115m}\text{Cd}$	$\sim 7 \times 10^8$	Molten Sn	plasma	2
	^{115}Ag	$\sim 1 \times 10^9$	<i>UC₂ or ThC</i>	<i>laser (Ag)</i>	
^{117}Cd (g.s.)	^{117}Ag (*)	$\sim 5 \times 10^8$	UC ₂ or ThC	laser (Ag)	4
^{111}Ag	^{111}Ag	$\sim 1 \times 10^8$	UC ₂ or ThC	laser (Ag)	2
^{140}La	$^{140}\text{LaO}^+$	$\sim 1 \times 10^8$	UC ₂ or ThC	Nb surface	2
	$^{140}\text{LaF}_2^+$ (†)	$\sim 1 \times 10^7$	<i>UC₂ + CF₄</i>	<i>Nb surface</i>	
^{143}Ce	^{143}Ce	$\sim 1 \times 10^8$	UC ₂ or ThC	Nb surface	1
^{153}Sm	^{153}Sm	$\sim 1 \times 10^8$	UC ₂ or ThC	Nb surface	1
^{52}Mn	^{52}Mn (‡)	$\sim 6 \times 10^7$	Nb-foil	laser (Mn)	2
	"	$\sim 10^8$ <i>estimated</i>	<i>ZrO₂</i>	<i>laser (Mn)</i>	
^{48}Cr	^{48}Cr (§)	$\sim 10^6$	Nb-foil	hot-plasma	2-test
					total: 26+2-test

(*) The implantation of ^{117}Ag maximises the ratio between $^{117}\text{Cd}/^{117m}\text{Cd}$, what is needed to optimise the PAC measurements, which are performed onto the 89.73keV- 344.4keV cascade on ^{117}In obtained from decay of ^{117}Cd (g.s.).

(†) The molecules LaO^+ or LaF_2^+ represent a way to get pure ^{140}La beams free of the long lived ^{140}Ba . The UC₂ or ThC targets are needed to reduce the radioactive isobar contamination from n-deficient lanthanides.

(‡) Data obtained from a test looking forward for the production of neutron deficient Mn isotopes from a Nb target. Most likely Mn isotopes can also be obtained from the ZrO target with the laser ion source.

(§) The availability of this beam would make possible that essential PAC experiments are performed. At the present status we ask for the possibility of considering 2 shifts for tests with the hot plasma ion source. However the Cr laser ion source, if developed as already required by other groups, could give about one order magnitude higher yields, estimated to be around 10^7 at/ μ C.

Due to the nature of the sample preparation [short time collection (5...20 min) of ^{111m}Cd for PAC measurements each 4h, or collections of long lived isotopes for PAC, EC and electrical/magnetic experiments], the beam time should be shared with other users with interests on the same type of target/ion-sources.

References

-
- [1] See, e.g., C. N. R. Rao and B. Raveau (eds.), *Colossal Magnetoresistance, Charge Ordering and Related Properties of Manganese Oxides* (1998), World Scientific, Singapore; Y. Tokura (ed.), *Colossal Magnetoresistive Oxides* (1999), Gordon & Breach, London; J. M. D. Coey, M. Viret, S. von Molnar, *Adv. In Phys.* 48 (1999) 167; Y. Tokura, Y. Tomioka, *J. Mag. Mag. Mat.* 200 (1999) 1.
 - [2] A. Moreo, S. Yunoki, E. Dagotto, *Science* 283 (1999) 2034.
 - [3] C. Zener, *Phys. Rev.* 82 (1951) 403; P. W. Anderson, H. Hasegawa, *Phys. Rev.* 100 (1955) 67.
 - [4] C. N. R. Rao and B. Raveau, *J. Phys. Cond. Matter* 12 (2000) R83; Y. Tokura, *Science* 288 (2000) 462.
 - [5] T. R. Mc Guire et al, *J. Appl. Phys* 79 (1996) 4549; S. Pignard et al., *J. Appl. Phys* 82 (1997) 4445; P. B. Tavares et al, *J. Appl. Phys* 85 (1999) 5411; R. Shreekala et al., *Appl. Phys. Lett.* 74 (1999) 1886.
 - [6] J. Topfer and J. B. Goodenough, *J. Sol. State Chem* 130 (1997) 117
 - [7] A. Goyal et al, *Appl. Phys. Lett.* 71 (1997) 2536; M. Rajeswari et al., *Appl. Phys. Lett.* 73 (1998) 2672.
 - [8] A. Barnabe et al., *Appl. Phys. Lett.* 71 (1997) 3907; Katsufuji et al, *J. Phys. Soc. Japan* 68 (1999) 1090; T. Kimura et al, *Phys. Rev. Lett.* 83 (1999) 3940.
 - [9] J. Rodriguez-Carvajal et al, *Phys. Rev. B* 57 (1998) R3189, Murakami et al, *Phys. Rev. Lett.* 81 (1998) 582, L. Vasiliu-Doloc et al, *Phys. Rev. Lett.* 83 (1999) 4393, Shimomura et al, *Phys. Rev. Lett.* 83 (1999) 4389, Yamamoto et al, *J. Phys. Soc. Japan* 68 (1999) 2538, M. Fath et al, *Science* 285 (1999) 1540; A. Lanzara et al, *Phys. Rev. Lett.* 81 (1998) 878.
 - [10] L. E. Rehn, *Nuc. Inst. Meth. B* 64 (1992) 161, S. B. Ogale et al. *J. Appl. Phys.* 84 (1998) 6255
 - [11] M. Nastasi in *Structure-Property Relationships in Surface-Modified Ceramics*, ed. C.j. McHargue (Kluwer, 1989) p. 477, R. Wang et al, *Phys. Rev. B* 47 (1993) 638, M. Urmacher and K-P. Lieb, *Z. Naturforsch.* 55a (2000) 90.
 - [12] M. Hervieu et al, *Phys. Rev. B* 60 (1999) R726, D. G. Naugle et al, *Int. J. Mod. Phys. B* 13 (1999) 3815

-
- [13] Y. Li et al., Phys. Rev. B51 (1995) 8498; idem, Appl. Phys. Lett. 68 (1996) 2738.
- [14] B. Hannoyer et al, Phys. Rev. B 61 (2000) 9613, M. Pissas et al, J. Appl. Phys. 81 (1997) 5770
- [15] G. Allodi et al, Phys. Rev. Lett. 81 (1998) 4736, G. Papavassiliou et al, Phys. Rev. Lett. 84 (2000) 761, Cz. Kapusta et al, Phys. Rev. Lett. 84 (2000) 4216, Y. Yoshinari et al, Phys. Rev. B 60 (1999) 9275
- [16] G. L. Catchen et al, Phys. Rev. B 54 (1996) R3679, R. L. Rasera and G. L. Catchen, Phys. Rev. B 58 (1998) 3218
- [17] J.G.Correia, Nucl. Inst. Meth. B 136-138 (1998) 736; B. Jonson, H.L. Ravn, and G. Walter, Nucl. Phys. News 3, 2 (1993) 5.
- [18] M. Sahana et al, Appl. Phys. Lett. 71 (1997) 2701
- [19] I. O. Troyanchuk et al, Phys. Stat. Sol. (a) 164 (1997) 821, J. P. Araujo et al, accepted for publication in J. Mag. Mag. Mat.
- [20] Th. Wichert, N. Achziger, H. Metzner and R. Sielemann, in Hyperfine Interaction of Defects in Semiconductors, edited by G. Langouche (Elsevier, Amsterdam, 1992).
- [21] U. Wahl, J.G. Correia, S. Cardoso, J.G. Marques, A. Vantomme, G. Langouche, and the ISOLDE collaboration, Nuclear Instruments and Methods B 136-138 (1998) 744-750
- [22] Z. Bukowsky et al, J. Appl. Phys 87 (2000) 5031
- [23] S. Pignard et al., J. Appl. Phys 82 (1997) 4445; P. B. Tavares et al, J. Appl. Phys 85 (1999) 5411; W. Prellier et al, Appl. Phys. Lett. 75 (1999) 1446
- [24] Y. Tomioka et al, Phys. Rev. B 53 (1996) 1689
- [25] A. Barnabe et al., Appl. Phys. Lett. 71 (1997) 3907;;
- [26] Katsufuji et al, J. Phys. Soc. Japan 68 (1999) 1090, T. Kimura et al, Phys. Rev. Lett. 83 (1999) 3940
- [27] T. Butz, S. Saibene, Th. Fraenzke and M. Weber, Nuc. Inst. Meth. A284 (1989) 417; W. Tröger, T. Butz, C. Lippert, B. Ctortecka, P. Schmidt, U. Schmidt, K.M. Comess and C.T. Walsh, Enzymatic Mercury Detoxification: The Regulatory Protein MerD, CERN/ISC 95-1, ISC/P69 (1994), IS348.
- [28] J.G. Correia, J.P. Araújo, J.G. Marques, A.R. Ramos, A.A. Melo, J.C. Soares, and the ISOLDE Collaboration, Zeitschrift für Naturforschung 55a (2000) 3